

FEM vibroacoustic analysis in the cabin of a regional turboprop aircraft

Maria Cinefra*, Sebastiano Passabi^a and Erasmo Carrera^b

Politecnico di Torino, Department of Mechanics and Aerospace Engineering, Italy

(Received November 22, 2017, Revised March 1, 2018, Accepted March 15, 2018)

Abstract. The main goal of this article is to validate a methodological process in Actran MSC Software, that is based on the Finite Element Method, to evaluate the comfort in the cabin of a regional aircraft and to study the noise and vibrations reduction through the fuselage by the use of innovative materials. In the preliminary work phase, the CAD model of a fuselage section was created representing the typical features and dimensions of an airplane for regional flights. Subsequently, this model has been imported in Actran and the Sound Pressure Level (SPL) inside the cabin has been analyzed; moreover, the noise reduction through the fuselage has been evaluated. An important investigation and data collection has been carried out for the study of the aircraft cabin to make it as close as possible to a real problem, both in geometry and in materials. The mesh of the structure has been built from the CAD model and has been simplified in order to reduce the number of degrees of freedom. Finally, different fuselage configurations in terms of materials are compared: in particular, aluminum, composite and sandwich material with composite skins and poroelastic core are considered.

Keywords: FEM; vibroacoustic analysis; noise reduction; sound pressure level; cabin comfort

1. Introduction

The purpose of this work is to drive innovative technologies, in terms of processes and materials, suitable for the fuselage of a regional aircraft in order to achieve improvements to the problem of noise and vibrations in the cabin, according to the studies by Rayleigh (1877) and Beranek (1960).

In general, the aircraft requirements are originated by:

- regulations (i.e., FAR, EASA) issued by the competent Aviation Authority; aircraft design and production must be compliant with them in order for the aircraft to be certified and so to be “airworthy”;
- customer needs identified by the marketing analysts and forwarded to the design offices;
- benchmarking of competitors.

Moving onto specific noise aspects, it is worth mentioning that regulations like FAR and EASA, in the field of aircraft design and production, mainly consist in safety standards, although

*Corresponding author, Associate Professor, E-mail: maria.cinefra@polito.it

^aStudent, E-mail: sebastiano.passabi@gmail.com

^bFull Professor, E-mail: erasmo.carrera@polito.it

the FAR do have a part devoted to environmental noise, as exposed in the work by Willshire and Stephens (1998) and ICAO annex 16 (2011). Hence, these regulations do not have quantified internal noise requirements, but only qualitative indications, which address safety aspects. For instance, it is requested that vibration and noise of cockpit equipment do not interfere with safe operation of the aircraft; this means that noise levels should allow safe, easy communication among pilots and flight crewmembers, but also that they should not cause distraction and so on. There are some military regulations that deal with internal noise; anyway, they concern the noise exposure hazard in aircraft cabin and cockpit and the speech intelligibility, but not the comfort aspects, which are mainly relevant in civil transport aviation, as discussed in the work by Beranek (2007).

Hence, interior noise requirements in civil transport aircraft (Wilby 1996) mainly derive from airline requests, which are made directly to aircraft manufacturers and that are based on passengers and cabin crew subjective response collected, for instance, by means of questionnaires as in the work by Pennig *et al.* (2012). Furthermore, the benchmarking of potential competitors is also very important, since new products are always expected to have a wide range of improved technical characteristics in order to enter the market successfully if compared to competitors already on the market. Nowadays the noise problem is attacking also small aircraft with classical configurations, as result of a lower technological progress in the field compared to the results of big airplanes and for the stringency of the aeronautical rules and local airport authorities which become with the time always more sensitive to the community noise level, as stated in ICAO Working Paper (2013) and CleanSky 2 (2014).

In the preliminary design phase, predictions of aircraft interior noise levels are made using simple approaches; the selection of the most appropriate tools and ways to carry out such predictions mainly depends on the aircraft type. In fact, noise sources that depend on aircraft type (particularly on propulsion type) influence noise energy frequency distribution (Bishop 1961). In this case an energy balance method will be used to make a preliminary assessment of interior noise levels expected in an aircraft cabin. For example, for a turboprop aircraft the near field noise excitation is mainly due to the propeller and therefore the major part of the acoustic energy is concentrated in the low frequency range (0-300 Hz). A major cause for increased noise transmission inside the cabin could be the coincidence between natural frequencies of the skin panels and the propeller tone frequencies. For last generation turboprop aircraft, in cruise conditions at least, the near field noise excitation is also due to Turbulent Boundary Layer, as studied in the report by Hayden *et al.* (1983), but this noise source is not considered in this work.

One more aspect has a fundamental importance to define the internal noise requirements and it is related to the acoustic treatments that are all the means/technical solutions that are installed on board to increase the noise reduction through the fuselage wall and to control the internal noise sources, as anticipated in the paper by Nichols *et al.* (1947). Some technologies proposed in the past are resumed in the work by Dobrzynski (2010). The following items contribute to reduce internal noise levels and hence may be regarded as noise treatments: thermo-acoustic blankets, skin damping, furnishing panels, mufflers, active noise control systems. The acoustic treatments configuration needs to be optimized taking into account different parameters, particularly the weight and the cost; an example is given by the honeycomb acoustic metamaterial proposed by Sui *et al.* (2015), which possesses lightweight and yet sound-proof properties. In particular, if one refers to a regional turboprop it can be considered that the mass of fuselage blankets, in percentage of the MEW, should be less than 1.4%. For these reasons, an acoustic configuration including an embedded layer of poro-elastic material between carbon-fiber panels has been considered in the

following analyses.

There is a lack of reliable and useful numerical models, valid for innovative configurations, able to predict the structural response and the radiated acoustic power. One can find some attempts in the automotive field, as presented by Yuksel *et al.* (2012). Thus, in the most of cases the experimental tests can certify the achievement of the desired performances. Nevertheless, the efforts in literature, directed toward some configurations, emerged during the years also due to the availability of composite materials, cannot be neglected: among them the works by Franco *et al.* (2011), Petrone *et al.* (2014), Arunkumar *et al.* (2016). A the state-of-the-art for the theoretical models able to predict the acoustic performance of the sandwich configurations, as well as the numerical modeling and experimental testing supporting these models, is provided in the article by D'Alessandro *et al.* (2013). The availability of a numerical tool, especially for regional aircraft which are subject to very different customer requests, is a fundamental need together with the confidence of the users of such tools who should have the ability for a correct, realistic interpretation of the results produced numerically. The basic assumptions rely on the diffuse acoustic field inside each elemental volume and on the acoustic energy balance among the input source and the exchange output among the different volumes. In parallel, the possibility of studying different materials is a driving factor for approaching the problem of the aircraft interior noise.

This paper will present the results obtained by numerical simulations performed with Actran, an MSC Software based on the finite element method. This is a powerful tool for the acoustic and vibroacoustic analysis of complex structures, accounting for various geometries, load conditions and materials. Moreover, this software allows different types of analyses to be performed, which have been validated through many applications presented in Workshop Series for Actran 17, Acoustics and Vibroacoustics Training (2016).

In this preliminary study, two different methodological approaches are considered, according to the available sources and the required solutions: diffusion sound field (DSF), that is the study of noise reduction (NR) inside a section of airplane cabin using a sampled random diffuse field; and spherical source, that is the study of the sound pressure level (SPL) transmitted into an airplane passenger ear by a spherical source that simulates the engine. In accordance with MSC Software tools, this work focuses on a general methodology to limit the complexity of the application, with the main goal to create a baseline method for the study of DSF/NR Energy Analysis and Engine – Spherical Sound Source. Different fuselage configurations are compared changing the materials: aluminum, composite and sandwich material with composite skins and poro-elastic core.

First, the Noise Reduction (NR) is computed in the cavity of the fuselage (this indicator shows how much the sound pressure level has decreased due to the presence of the structure and it is useful to evaluate the acoustic performances of different materials), then the SPL is evaluated in the cabin by considering an external spherical sound source that simulates the engine. Different fuselage configurations, in terms of materials used, are taken into account and the most promising solution is identified.

2. Fuselage study case

Exposure to noise inside the aircraft has always been a prevalent problem for pilots. Noise is produced by two principal sources, fuselage boundary layers and turbojet exhaust and four other relevant noises, turbomachinery, cabin conditioning and pressurization systems, structure-borne

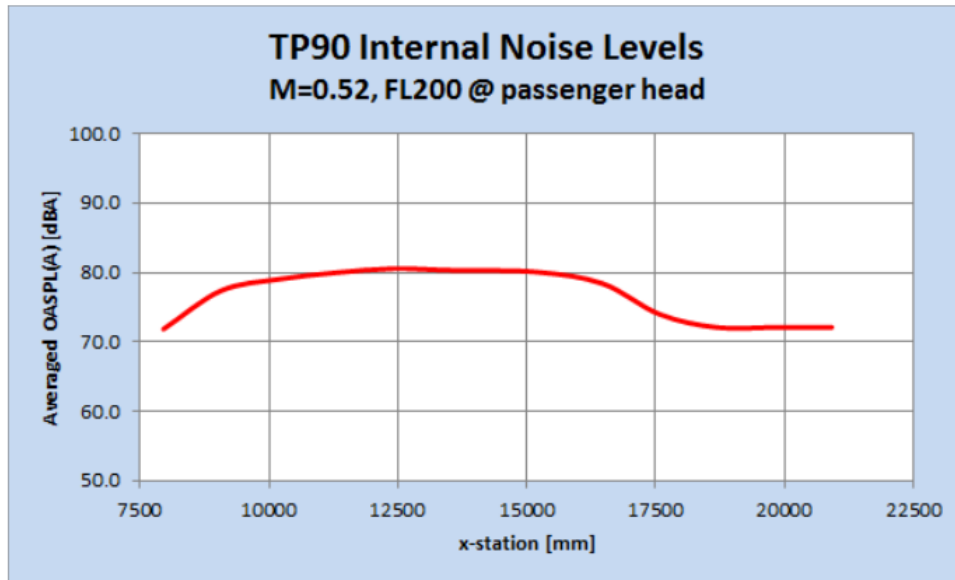


Fig. 1 Cabin noise levels

noise and aerodynamic flow. Other noise sources are masked by the ones mentioned before, as for example hydraulic and electrical actuators. Noise is transmitted to the cabin along airborne paths through the fuselage sidewall and along structure borne paths through the engine mounts or the wing structure. Each aircraft has its characteristics sounds used by pilots as a diagnostic system. As a reference value, jet cabins sound pressure level is comprised between 60 and 88 dB. Long noise exposure over 85 dB could cause hearing lost. Noise inside the cabin must be reduced not only for comfort: hearing damage, fatigue and reduction of concentration must be avoided, not only for the passengers but also for the pilots.

The following section intends to address the noise requirements for a regional turboprop aircraft, with respect to the cabin environment, which should drive future cabin design to provide comfort to the aircraft occupants. Taking into account that for a turbo-prop aircraft the near field noise excitation is mainly due to the propeller and therefore the major part of the acoustic energy is concentrated in the low frequency range (0-300 Hz), one more aspect which has fundamental importance in defining the internal noise requirements is related to the acoustic treatments, that are all the means/technical solutions adopted to increase the noise reduction of the fuselage wall.

2.1 Reference turboprop internal noise requirements

A single aisle regional aircraft with a medium capacity of 60-90 seats has been used as a reference to assess the methodologies presented in this work. Basically, noise requirements are strongly dependent on the type of aircraft, being linked to the aircraft operating conditions and characteristics (Mach number, flight altitude, type of engine, etc.). Typically, internal noise requirements for regional turboprop aircrafts address cruise and climb flight phases. Take-off condition can be noisier, but, given its limited time duration, it is usually not considered for noise requirements.

Generally, averaged levels are defined at seated passenger ear height and at aisle center. Also

different levels are taken into account in different fuselage regions (two or three maximum) at different longitudinal positions with respect to engine. In particular, we refer to the overall sound pressure level, OASPL, in the frequency range 50-10000 Hz, A-weighted (see Fig. 1).

The following simplified approach is followed:

- propellers have been considered as the major noise source;
- Turbulent Boundary Layer (TBL) noise and the internal noise sources have been neglected;
- cabin sound absorption is simulated addressing fuselage walls, carpet and seats absorption characteristics.

For a regional turboprop in cruise conditions the averaged interior noise level at seated ear height and at center aisle should not exceed 74 dBA, eventually varying along with fuselage station.

In this study case, for a limit of computational resource, it was created a simple model of a semi-section of fuselage of 1 meter of length. The model considers the worst acoustic case in the cabin, that is the fuselage tract with nearest seats to engine.

2.2 Methodological approach in Actran

Two different kinds of methodological study are considered, according to the resources available and the solutions required:

1. DIFFUSE SOUND FIELD with the study of transmission loss/noise reduction inside a section of airplane cabin using a random diffuse sound field.

Diffuse sound field definition: sound field in which the time average of the mean square sound pressure is everywhere the same and the flow of acoustic energy in all directions is equally probable. Such, a diffuse acoustic field is usually produced experimentally by activating acoustic source in a reverberant chamber, the multiple reflections along boundary walls lead to a diffuse field.

2. SPHERICAL SOURCE: study of sound pressure level transmitted to the airplane passenger ears by a spherical source that simulates the engine.

A point source of (complex) amplitude A , located at point P , generates an incident sound field P_i defined by

$$P_i = A \frac{e^{-ikr}}{r}$$

where r is the distance between P and the point where the incident pressure is computed, while k is the wave number; f is the frequency and c the sound speed. A spherical source is entirely determined by its amplitude A and its position P .

In the first case, an analysis at component level is presented; in the second case, a spherical source is used for an analysis at system level of the SLP in the whole model.

3. FEM model

3.1 Cabin definition

Having analyzed the parameters for the analysis of the comfort level in the fuselage of the regional aircraft we have chosen, the model was created in CAD (Fig. 2). Considering an

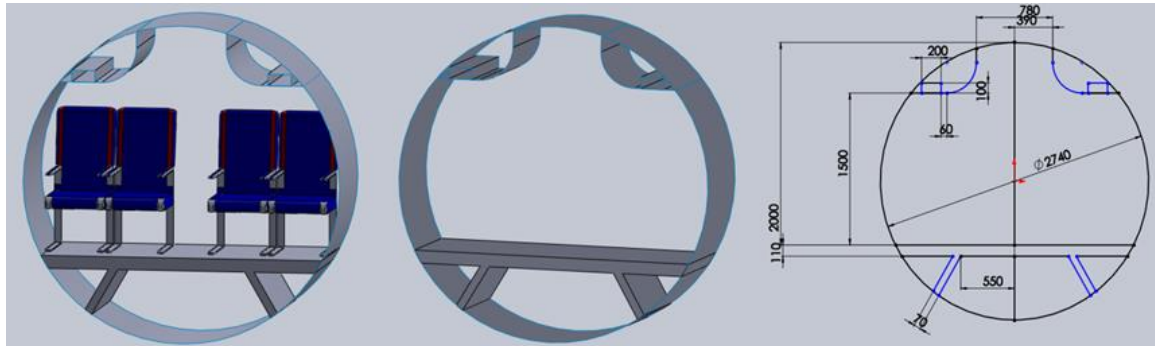


Fig. 2 CAD model of the fuselage trunk (dimensions are given in [mm])

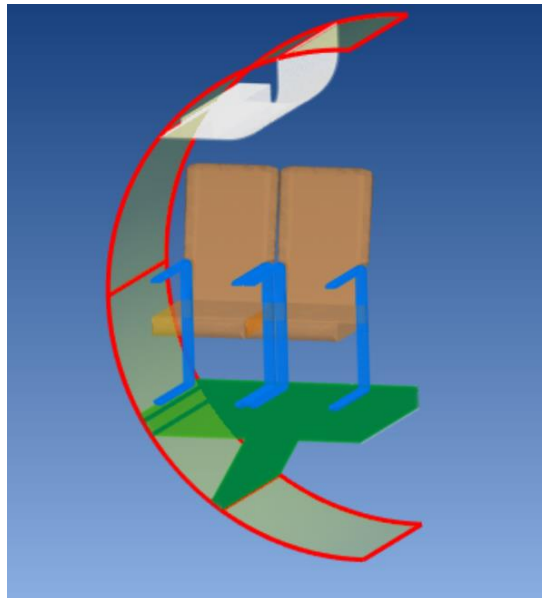


Fig. 3 Mesh of the fuselage semi-section

hypothetical fuselage trunk and selecting a circular section model with four seats for sitting, we finally chose to work only with half of the fuselage trunk because of its symmetry.

Once CAD model of the fuselage trunk was created, the software Apex MSC Software transformed the CAD file into a mesh file with format *.bdf. Inaccuracies have been manually corrected in order to make the model recognizable by Actran (Fig. 3).

The model consists in 2420 1D elements, 177329 2D elements, 478375 3D elements and 384014 nodes. The mean length of the elements is $1.32e-2$ m. Modal analysis and direct frequency response analysis have been performed in order to evaluate noise reduction and sound pressure level, as in the following sections.

3.2 Materials database

Following, Tables 1-9 contain the mechanical and physical properties of the materials used for the different items of the cabin model.

Table 1 Material and geometrical properties of the fuselage stiffenings (from Actran database)

Stiffenings	
Solid Density ρ	2780 Kg/m ³
Poisson Ratio ν	0.3
Elongation Modulus E	72400 MPa
Shear Modulus G	27218 MPa
Area	7.8e-05 m ²
Cross Section Inertia Xx	1.24850e-08 kg/m ²
Cross Section Inertia Xy	0 kg/m ²
Cross Section Inertia Yy	5.80282e-10 kg/m ²
C _g Offset X	0.0185
C _g Offset Y	0.0
Shear Factor X	0.6
Shear Factor Y	0.35
Shear Offset X	0.0185
Shear Offset Y	0.0
Inertia Torsional	5.85e-11 kg/m ²

Table 2 Properties of the aluminum material used for the fuselage wall, floor and reinforcement

Aluminum	
Young Modulus E	70000 MPa
Poisson Ratio ν	0.3
Solid Density ρ	2700 Kg/m ³

Table 3 Properties of the composite laminate used for the fuselage wall, floor and reinforcement (when used for the stowage bin and the backrest of seats, the lower thickness is considered)

Composite			
Layer	Material	Thickness [m]	Angle
1	Transverse Isotropic Solid	0,001 / 0,0005	90°
2	Transverse Isotropic Solid	0,001 / 0,0005	45°
3	Transverse Isotropic Solid	0,001 / 0,0005	0°
4	Transverse Isotropic Solid	0,001 / 0,0005	0°
5	Transverse Isotropic Solid	0,001 / 0,0005	135°
6	Transverse Isotropic Solid	0,001 / 0,0005	135°
7	Transverse Isotropic Solid	0,001 / 0,0005	90°
8	Transverse Isotropic Solid	0,001 / 0,0005	90°

3.3 Fuselage configurations

3.3.1 Upper engine aluminum internal fuselage (UAFI)

In this study case, a single aluminum layer of 1 mm thickness was assigned to the fuselage. In

the model, there is a second outer layer of the fuselage (the distance between the midsurfaces of the two layers is taken 10 cm) but in this configuration it has not been associated with any component and domain, then the software doesn't take it into account in the calculation process. The aluminum material of the internal fuselage layer was employed also for the floor and its reinforcement, while the isotropic composite material was used for the stowage bin and the backrest of the seats, the 3D porous material for the carpet of the floor and the foam for the seat cushions. In the mesh corresponding to the external volume around the sound source engine and the internal one to the fuselage, it has been assigned the finite fluid properties of air.

3.3.2 Upper engine composite internal fuselage (UCFI)

The properties of the composite material are taken directly from the database of Actran software. This facilitated the modeling and the run of the computation, giving one more test available for the following comparisons. The composite material has been associated to the items that in the previous configuration were made of aluminum. A single internal layer of fuselage is considered.

3.3.3 Upper engine cross-ply composite internal fuselage (UCCFI)

In this configuration, the cross-ply composite material has been associated to the items that in the previous configuration were made with Actran composite.

Table 4 Properties of the transverse isotropic material used for the composite laminate of Table 3 (from Actran database)

Transverse Isotropic Solid	
Inplane Poisson Ratio ν_{LT}	0.25
Normal Poisson Ratio ν_{TT}	0
Normal Modulus E_L	145000 MPa
Solid Density ρ	1700 Kg/m ³
Inplane E Modulus E_T	10000 MPa
Normal S Modulus G_{LT}	4800 MPa

Table 5 Properties of the cross-ply composite used for the fuselage wall, floor and reinforcement

Cross-ply Composite			
Layer	Material	Thickness [m]	Angle
1	Orthotropic Solid	0.0003	0°
2	Orthotropic Solid	0.0003	90°
3	Orthotropic Solid	0.0003	0°
4	Orthotropic Solid	0.0003	90°
5	Orthotropic Solid	0.0003	0°
6	Orthotropic Solid	0.0003	90°
7	Orthotropic Solid	0.0003	0°
8	Orthotropic Solid	0.0003	90°
9	Orthotropic Solid	0.0003	0°

Table 6 Properties of the transverse orthotropic material used for the composite of Table 5

Orthotropic Solid	
Young modulus E_1	132380 MPa
Young modulus E_2	10760 MPa
Young modulus E_3	10760 MPa
Poisson ratio ν_{13}	0.24
Poisson ratio ν_{12}	0.24
Poisson ratio ν_{23}	0.49
Shear modulus G_{13}	5650 MPa
Shear modulus G_{12}	5650 MPa
Shear modulus G_{23}	3610 MPa
Solid Density ρ	1578 Kg/m ³

Table 7 Properties of the porous material used for the core of the fuselage wall

Polyimide	
Flow Resistivity σ	2e-10
Biot Factor B_i	0.45
Viscosity μ	1.82e-05 Pa·s
Young Modulus E	60000+20i Pa
Solid Density ρ	9.6 Kg/m ³
Poisson Ratio ν	0.45
C_p	1004.0
C_v	716.0
Tortuosity τ	3.25
Fluid Density ρ_f	1.225 Kg/m ³
Thermal Conductivity λ	0.0256 W/(mK)
Fluid Bulk Modulus K_f	140000 Pa
Porosity ϕ	0.45 V_{por}/V_{tot}

Table 8 Properties of the material used for the carpet of the floor (from Actran database)

Porous material	
Flow Resistivity σ	3000
Viscous Length Λ	3e-05 m
Viscosity μ	1.821e-05 Pa·s
Young Modulus E	192000+ 24960i Pa
Solid Density ρ	827 Kg/m ³
Poisson Ratio ν	0.23
Thermal Length Γ	8e-05
Tortuosity τ	1.05
Fluid Density ρ_f	1.225 Kg/m ³
Thermal Conductivity λ	0.02561 W/(mK)
Porosity ϕ	0.94 V_{por}/V_{tot}

Table 9 Properties of the material used for the seat cushions

Foam	
Flow Resistivity σ	22000
Biot Factor Bi	1.0
Viscous Length Λ	1.7e-05 m
Viscosity μ	1.82e-05 Pa·s
Young Modulus E	192000+24960i Pa
Solid Density ρ	827 Kg/m ³
Poisson Ratio ν	0.23
Thermal Length Γ	4e-05 m
Cp	1004 J/K·kg
Cv	716
Tortuosity τ	1.38
Fluid Density ρ_f	1.225 Kg/m ³
Thermal Conductivity λ	0.0256 W/(mK)
Fluid Bulk Modulus Kf	101300
Porosity ϕ	0.97 pori/Vtot

3.3.4 Upper engine cross-ply composite external fuselage (UCCFE)

In this case, the same configuration of the previous case has been used, but the outer layer of the fuselage is included. The cross-ply composite is assigned also to the outer layer and an acoustic volume of air has been associated to the volume included between the two shells of the fuselage wall.

3.3.5 Upper engine cross-ply composite with polyimide external fuselage (META)

This particular configuration has been analyzed in order to test the absorption properties of a new porous material, such as the Polyimide. The Polyimide substitutes the volume of air between the two cross-ply composite layers in the previous model. In this way, a sort of sandwich structure is obtained with very stiff skins and a viscoelastic soft core. This last, being porous, provide a good sound absorption at high frequencies. Since the use of very different materials in the same structure is the basic idea of the metamaterials design and the authors are studying a metamaterial configuration in which the absorption of the poro-elastic material in the low-frequency range is improved by adding metallic inclusions, according to the work presented by Sagle (2014), this fuselage configuration is indicated with the acronym META.

4. Noise reduction (NR)

An analysis at component level is here presented. A single component, that is the semi-circular panel of the fuselage (Fig. 4), is studied. The advantages of this kind of analysis are the following:

- it is easier to find a correlation with the experimental results (less uncertainties)
- provides structure response to higher frequencies;
- provides immediate component design guidelines.

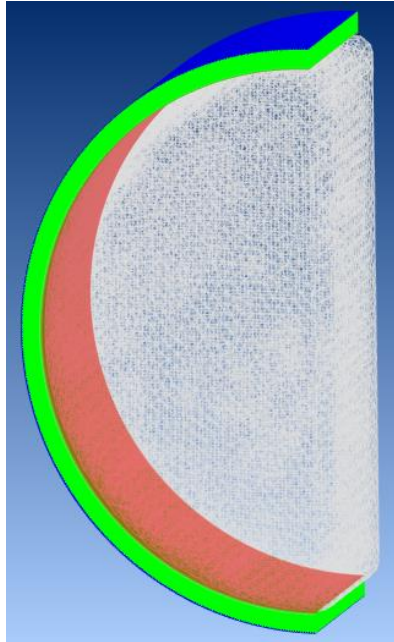


Fig. 4 Mesh of the semi-circular panel of the fuselage (stiffenings are included)

Any plotted function in PLT Viewer has a type, characterizing the nature of its underlying data. Depending on this function data type, the corresponding octave/mean octave data will be computed in a different way. Among the data type available in PLT Viewer, there are;

- dB: function data expressed in decibels [dB] scale (logarithmic scale). Any dB operator, such as dB_pressure, dB_power, etc., applied to a data vector will lead to a function with underlying dB data type;
- TL: function data corresponding to a Transmission Loss (TL) or Noise Reduction (NR) indicator. TL and NR operators applied to a data vector will lead to a function with underlying TL data type.

In addition to the function data type, there is also a dB reference value associated to a function data. This parameter is used when the data type is dB. In such a case, PLT Viewer has to determine if the data is linear dB data (dB_pressure) or quadratic dB data (dB_power), because the dB reference is not the same for these two different types of data. Let's consider the general expression for converting pressure quantity to dB units

$$p_{dB} = 20 \log \left(\frac{p}{p_{ref}} \right)$$

In the above expression, there is a given reference pressure level. The dB reference level for the pressure is $2 \cdot 10^{-5}$ (this is the default dB reference of any function created in PLT Viewer; this value can be changed in PLT Viewer Settings window), while dB reference value for the power is $1 \cdot 10^{-12}$.

The Transmission Loss indicates the level of the sound pressure transmission loss by calculating how much energy is lost through obstacles or air volumes, unlike the noise reduction

that analyzes the decibel level by considering the amount of sound pressure. In the aeronautical field, the Noise Reduction is preferred to the Transmission Loss: the analysis is set in the same manner except for the power evaluation, that is not required in the NR which concerns only the pressure, not the energy.

The noise reduction is defined as

$$NR = 10 \log \left(\frac{\frac{1}{S_{inc}} \int |p_{inc}|^2 ds}{\frac{1}{V_{cav}} \int |p_{cav}|^2 dv} \right) = 10 \log \left(\frac{|p_{inc}|^2}{|p_{cav}|^2} \right)$$

Since for interior cabin noise applications the pressure values inside the fuselage are more representative, the NR is calculated as the mean square pressure in the cavity of the fuselage. The displacements and rotations on the boundaries of the fuselage panel have been blocked.

As the floor, reinforcement, seats and stowage bin are not included in the model, the results could not be much reliable, but this analysis is performed only to compare the acoustic efficiency of the different fuselage configurations.

Fig. 5 shows and compares the results obtained in terms of NR for three different fuselage configurations: UCCFI, UCCFE and META.

In the first analysis, we consider the fuselage configuration UCCFI. In order to run the NR analysis, the internal volume of the cabin has been meshed. Fig. 6(a) shows an example of displacements map at frequency 490 Hz. To create the pressure map of Fig. 6(b), a 2D mesh across the mid-section of the fuselage trunk has been used.

Analyzing the curve of Fig. 5 relative to UCCFI configuration, we note that the panel maintains a mean reduction of approximately 25 dB over 1000 Hz and other minimums are observed at low frequencies of 100, 200, 340, 460, 490 and 570 Hz.

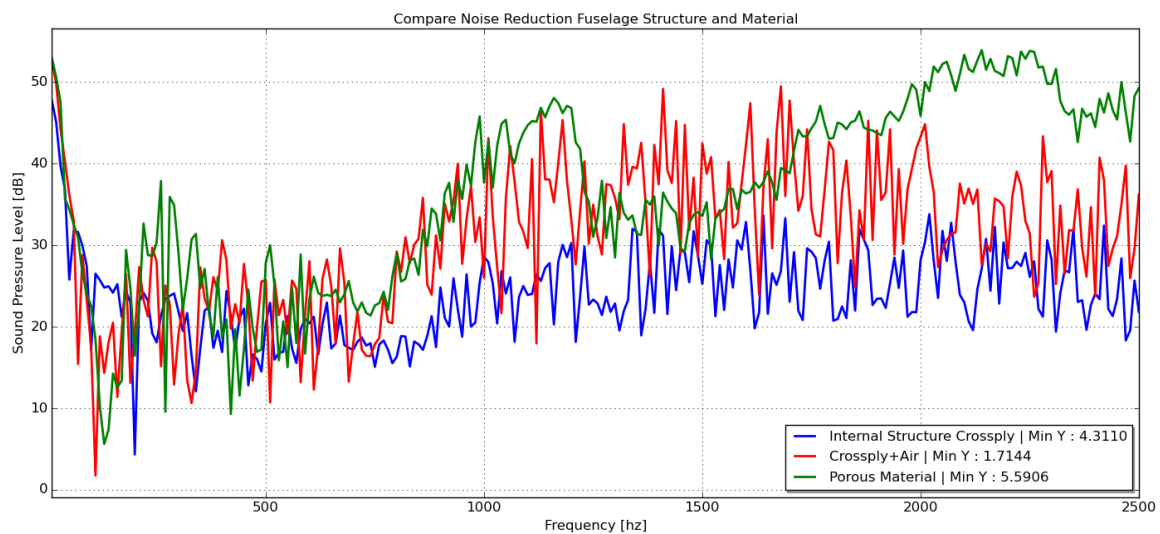


Fig. 5 NR – Comparison of configurations UCCFI, UCCFE and META

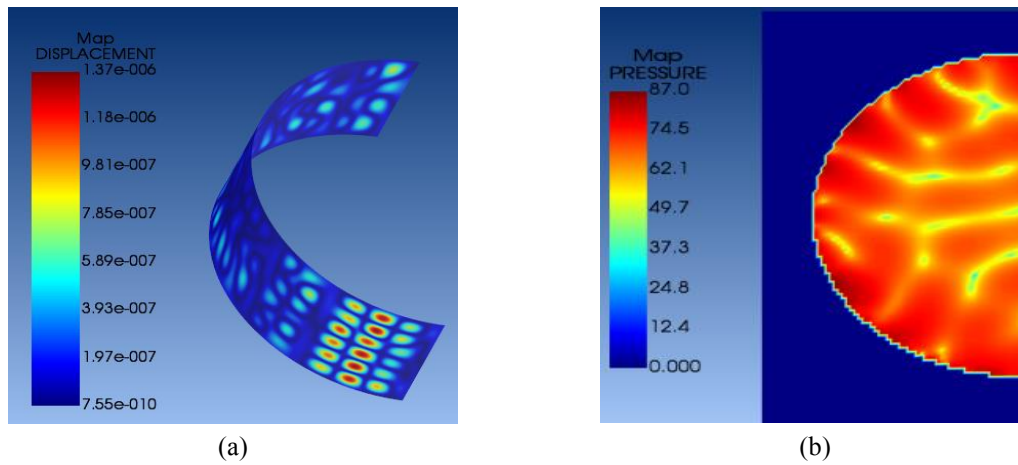


Fig. 6 NR – Cross-ply composite fuselage (UCFI) Displacement (left) and pressure (right) maps

Then, configuration UCCFE is analyzed. One can immediately note that the presence of an air gap between the two panels involves a significant improvement of the Noise Reduction, especially at high frequencies where the average of the NR is around 30 dB. The minimum NR conditions are observed at the low frequencies of 70, 110, 330, 510, 1120 Hz.

Finally, the META configuration is taken into account. In this case, a significant improvement to the NR at higher frequencies (over 1500 Hz) with a mean minimum of about 40 dB, is given by the addition of the Polyimide between the two composite fuselage shells. Even at low frequencies one can notice some improvements, but still important minimums can be measured at 130, 270, 420 and 550 Hz.

Comparing the three tests, we can conclude that the presence of a poro-elastic material, such as Polyimide, improves the reduction of perceived noise inside the fuselage.

Analyzing the results carefully, one can note that the porous material increases the noise reduction at middle frequencies up to about 1250 Hz, even if there are two minimums at 270 and 420 Hz that are lower than composite material. Another frequency range where the porous material is not very efficient goes from 1250 to 1750 Hz. In this range, the structure with an air gap performs better. Anyway, at very high frequencies the porous material provides the higher noise reduction.

5. Sound pressure level (SPL)

The Direct Frequency Response (DFR) is a computation procedure used to compute the response of an acoustic, vibroacoustic or aero-acoustic system to a specific excitation in physical coordinates. This is the most common Actran analysis type. We expose then every case analyzed with DFR.

Since we need to analyze only half trunk of the fuselage, precisely the most close to the engine, we chose to consider the classic configuration of a turboprop aircraft with high wing. The changes that are going to be performed are the choice of materials for the structure of the fuselage and the possibility to have an outer covering of the same structure. Once all the structural tests are performed to ensure the correct response of the model, we proceed with the analysis of the different fuselage configurations.

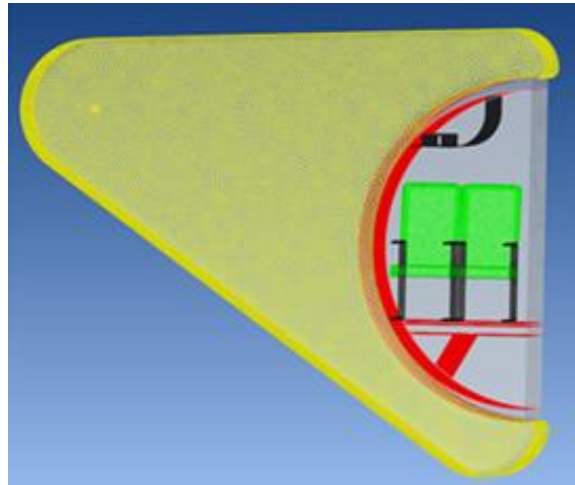


Fig. 7 Fuselage trunk with sound spherical source

In DFR, the spherical source simulates the presence of an engine (Fig. 7), positioned under the wing of a turboprop aircraft with high wing configuration. It must be supported by a volume mesh. This volume identifies the air around the engine and the air inside the cabin, as means of propagation of sound.

Once all the mesh types are loaded, we can associate the following properties and boundary conditions to the complete model.

- Air cavity: the properties of finite air fluid are associated to each empty volume.
- Material volume: the properties of the porous material are associated to the volumes of the seats, carpet and the core of the configuration META.
- Thin shell: the materials and relative thicknesses are associated to the surfaces.
- Interface between coupling surfaces: the coupling between surfaces with different meshes is accomplished with precise tolerance.
- Infinite acoustic: a property of infinite elements is associated to the outer surfaces that delimit the entire model in order to eliminate the sound reflection.
- All the displacements and rotations are blocked on the boundaries of the fuselage panel.
- Spherical source: the engine is simulated by an external spherical sound source.

For the post-processing, the following elements are considered.

- Microphones with point evaluation associated to the Frequency Response Function (FRF) output. These are positioned as follows:
 - three at standing position in the aisle, taking into account the average height of the European population (center corridor 1.65 m, 1.70 m and 1.75 m from the floor);
 - two at ears positions for the window seat;
 - two at ears positions for the aisle seat;
 - a sphere microphone for the possible head movement at the window seat;
 - a sphere microphone for the possible head movement at the aisle seat.
- Output map associated to the domains of the fuselage, floor and reinforcement that provides information about the displacements of the structure (example in Fig. 9).
- Field map associated to a longitudinal and transversal plane that provides the variation of pressure level sound across the fuselage (example in Fig. 9).

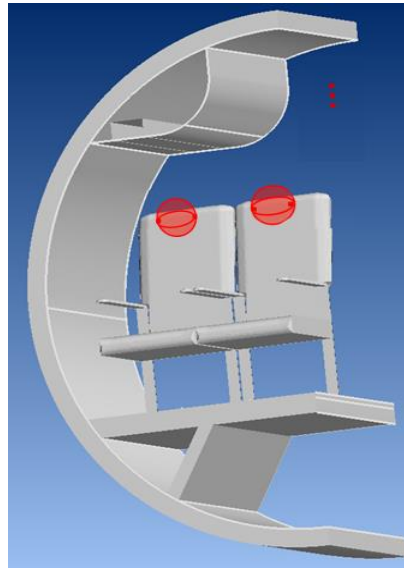


Fig. 8 Microphones positions

All the input files, with format *.edat, required a computing power of about 70 GB of RAM, on a server with 190 GB of RAM and 16 CPUs. Three parallel calculations have been used, so the computation time has been reduced to approximately 12 hours.

The results obtained in Fig. 9 are provided in files with format *.plt, in which the PLT Viewer of Actran graphically shows the pressure trend and amplitude of displacements for each microphone and point load previously set in the input file. The data analysis was visually carried out through them, looking for the resonance peaks of each configuration at specific frequencies. Actran output maps are useful to identify critical regions to be improved from an acoustical point of view: for example, by redefining the materials, or changing the disposition of structural elements (reinforcements), etc. They also allow the acoustic conditions to be predicted at any point of the model and to take action where needed.

In the model, there are multiple point load and microphones (Fig. 8) which detect the number of decibels inside the fuselage. Since the number of microphones is high, the different regions are computed using the mean quadratic pressure.

The quadratic means have been obtained by the equation

$$p_{rms}^2 = p_1^2 + p_2^2 + p_3^2 + \dots$$

The mean square sound pressure results are given by the combination of two or more pure tones of different amplitudes $p_1, p_2, p_3 \dots p_N$ at different frequencies $f_1, f_2, f_3 \dots f_N$. Therefore, taking as reference values the amplitudes at each frequency for every microphone the mean value is calculated, then the average amplitudes at each frequency are converted into decibels for the Sound Pressure Level through the equation:

$$SPL_p = 10 \log \left[\frac{p(t)}{P_{ref}} \right]^2 = 20 \log \frac{p(t)}{P_{ref}}$$

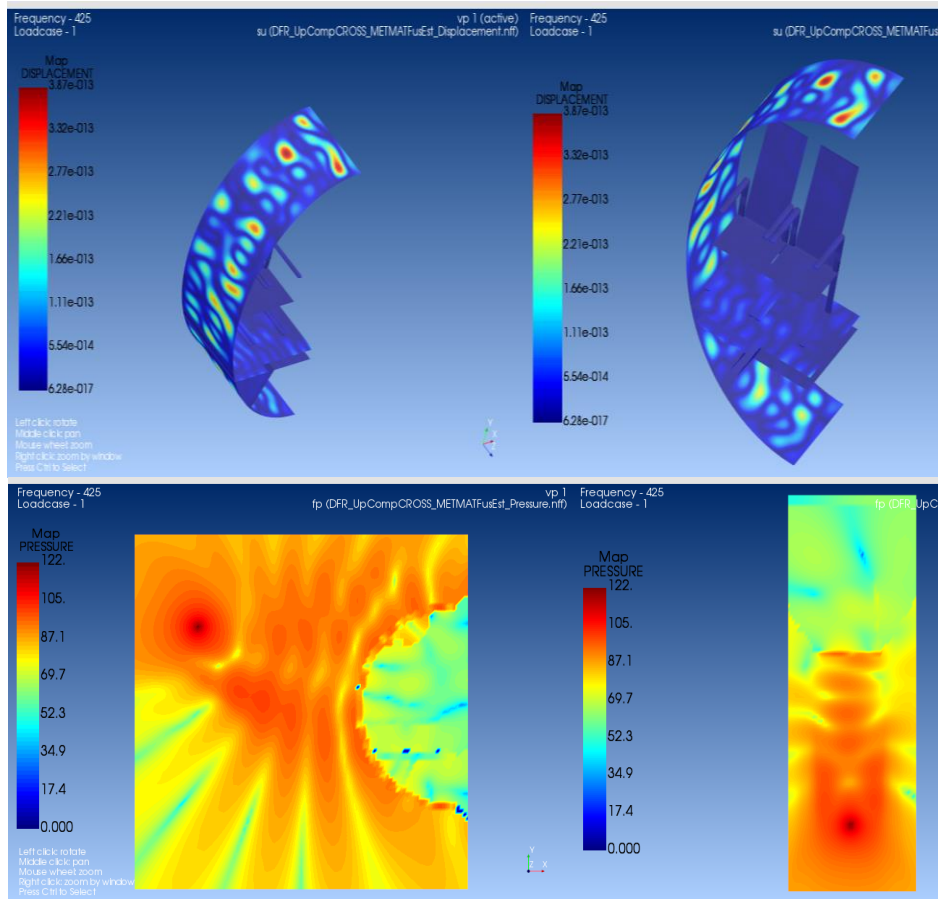


Fig. 9 (up) Output map and (down) field map at 425 Hz for the META configuration

p_{ref} is reference sound pressure, standardized at 2×10^{-5} N/m² (20 μ Pa) for airborne sound and $p(t)$ is the instantaneous sound pressure. This last is then converted into dBA, A-weighted sound pressure level SPL_A , which is the actual value of decibels perceived by man. In this case, the following equation is used

$$SPL_A = 10 \log \left[\frac{p_A(t)}{p_{ref}} \right]^2 \quad [\text{dB}]$$

where $p_A(t)$ is the instantaneous sound pressure measured using the standard frequency-weighting A, according to the book by Beranek and Istvan (2006) (see Table 10).

Five cases are analyzed below to detect the variations in sound pressure level inside the fuselage.

5.1 Results

5.1.1 Microphones of isle

For this case the results are provided in Fig. 10. In this condition, one can note that for low frequencies, up to 400 Hz, the chosen materials keep a limit level of sound pressure level of 76,5

Table 10 A-weighting for sound pressure level

Frequency [Hz]	A-Weighting Relative Response [dBA]
10	-70.4
12.5	-63.4
16	-56.7
20	-50.5
25	-44.7
31.5	-39.4
40	-34.6
50	-30.2
63	-26.2
80	-22.5
100	-19.1
125	-16.1
160	-13.4
200	-10.9
250	-8.9
315	-6.6
400	-4.8
500	-3.2
630	-1.9
800	-0.8
1000	0
1250	+0.6
1600	+1.0
2000	+1.2
2500	+1.3
3150	+1.2
4000	+1.0
5000	+0.5
6300	-0.1
8000	-1.1
10000	-2.5
12500	-4.3
16000	-6.6
20000	-9.3

dBA (74 dBA + 2,5 dBA due to the wing effect). This level is acceptable for a good acoustic comfort in the cabin, but the composite materials fail to maintain a sufficiently low noise level over the 865 Hz.

Each material behaves differently depending on the frequencies: the porous material does not

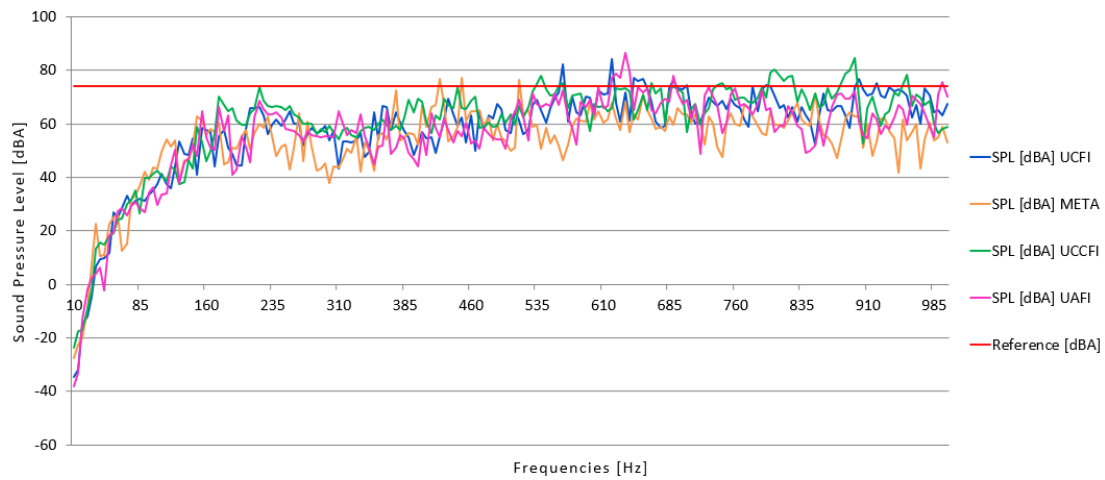


Fig. 10 Trend of sound pressure level in the isle

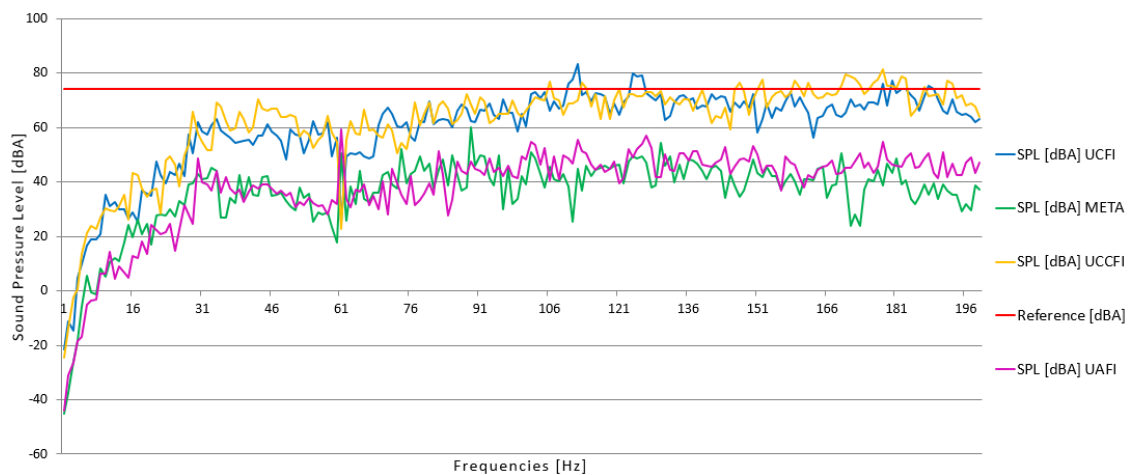


Fig. 11 Trend of sound pressure level at the ears of the window seat

respond well at medium-low frequencies of 415 and 525 Hz. The highest peaks occur in the aluminum fuselage at 635 Hz and for the cross-ply fuselage at 895 Hz.

In general, the results with lower trends are given by aluminum or porous material.

5.1.2 Microphones at ears of window seat

The results do not change much with respect to the previous case (Fig. 11). One can immediately note that the configurations with composite materials tend to exceed the limit of 74 dBA at 815 Hz for the UFCCI configuration and 915 Hz for the UFCI one.

The lower sound pressure levels are obtained META configuration followed by the fuselage of aluminum. This last two materials do not present resonance peaks over 76,5 dBA, while the UFCI shows resonance peaks at 625 and 905 Hz and the UFCCI at 535 and 895. In these conditions, one can see from the Fig. 12 how the increase in the frequencies overlap of the sound waves leads to a decrease of the internal comfort of the fuselage, particularly in points more distant from the stiffenings.

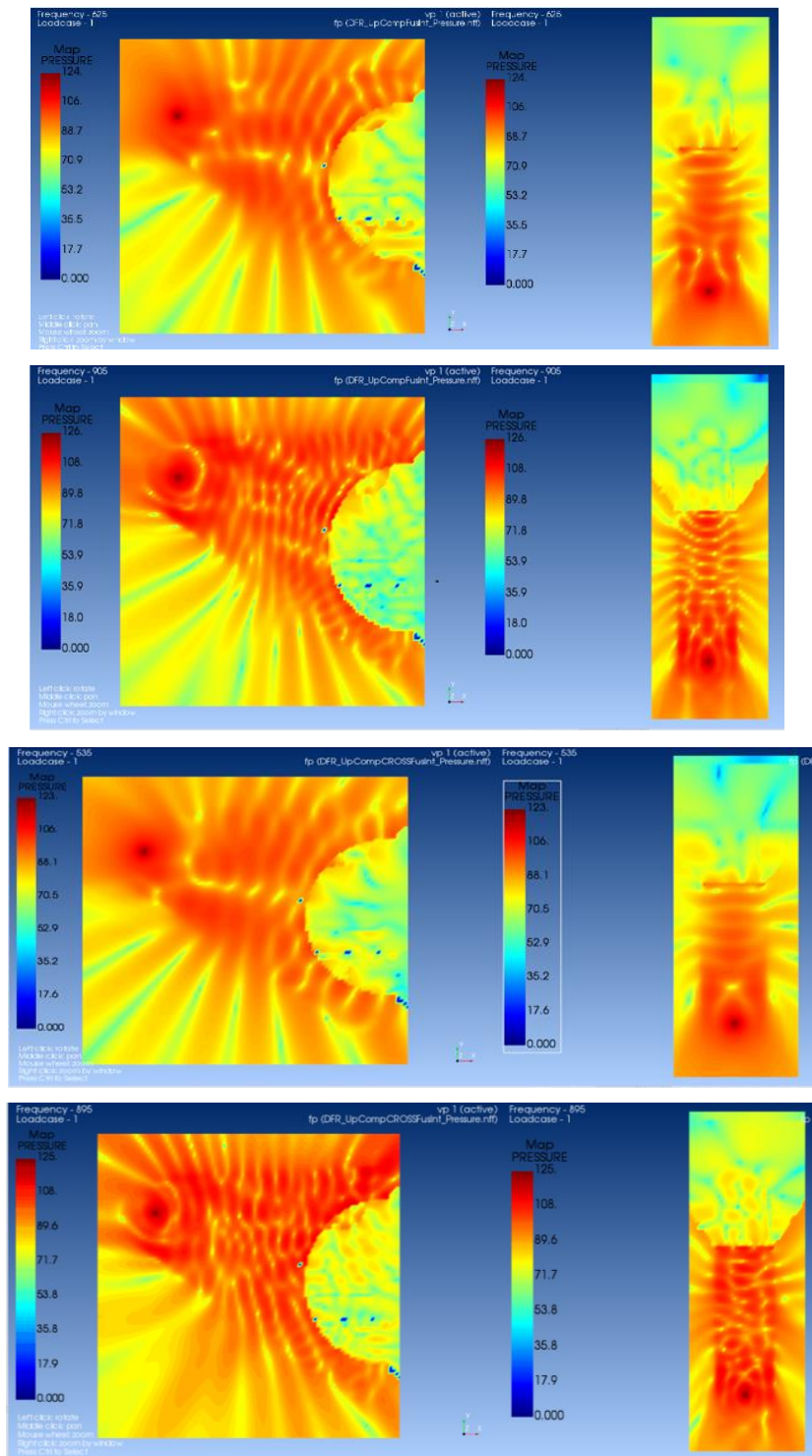


Fig. 12 Field maps of UFCI configuration at 625 Hz (first) and 905 Hz (second) and UFCCI configuration at 535 Hz (third) and 895 (fourth)

5.1.3 Microphones at ears of isle seat

Also in this case (Fig. 13), the best response is given by the aluminum fuselage and the configuration with porous material.

The configurations with composite materials provide the highest SPL, which exceeds the maximum limit at 890 Hz and the fuselage with porous core shows over limit resonance peaks at medium-low frequencies of 450 and 515 Hz.

5.1.4 Sphere microphone at the head of window seat

In this case (Fig. 14), one can note that for all the configurations, except for the case in which the porous material is used, the limit of 76,5 dBA is exceeded at high frequencies, probably because a greater number of microphones is considered at different points of the seat to simulate the movements of the head.

The worst acoustic conditions are again associated to the composite configurations and the META shows a resonance peak at 450 Hz. While the fuselage with aluminum panel should be revised to 725 and 755 Hz where two resonance peaks are present.

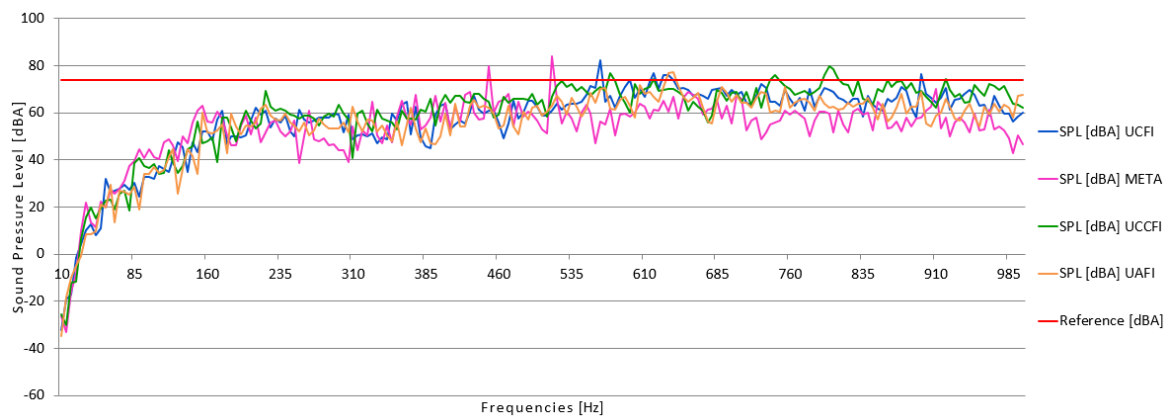


Fig. 13 Trend of sound pressure level at the ears of the isle seat

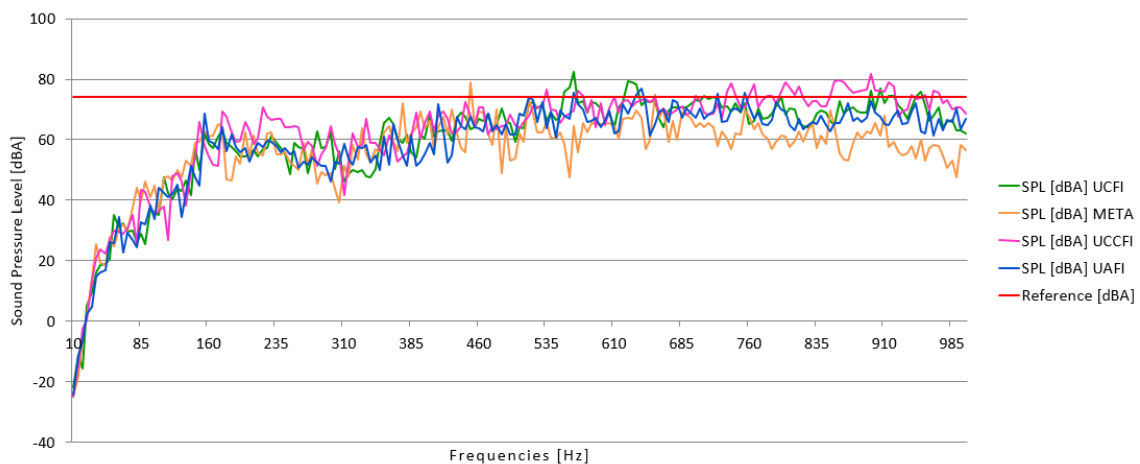


Fig. 14 Trend of sound pressure level at the head of the window seat

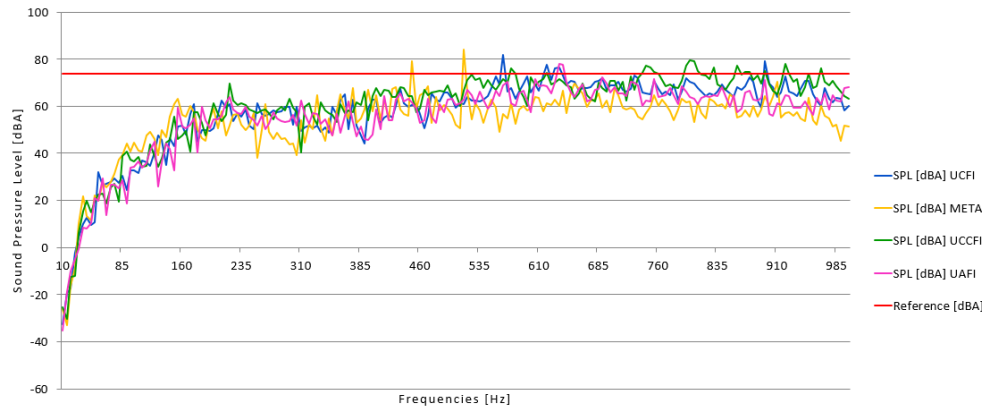


Fig. 15 Trend of sound pressure level at the head of the isle seat

5.1.5 Sphere microphone at the head of isle seat

This comparison (Fig. 15) confirms the comments of the previous cases. The best acoustic conditions, that is the lower sound pressure level trend is given by META configuration and the aluminum SPL decreases slightly with respect to the previous case, probably because the microphones are more distant from the fuselage. Finally, the porous material fuselage presents resonance peaks in the medium-low frequencies, as before.

6. Conclusions

This work was focused in performing two types of analysis: the first one at the component level and the second one at the system level. In the analysis at the component level, being the calculation faster, it was easier to compute and understand how the specific part behaves and it was possible to obtain results at higher frequencies. At system level, the Sound Level Pressure perceived by the passengers can be predicted; moreover, the structural response of the aircraft can be evaluated and then improved.

Regarding the analysis at component level, the panel of fuselage was analyzed, trying to understand which material provides the highest noise reduction inside the cabin. As expected, the fuselage with composite faces and poro-elastic core showed excellent results for almost all frequencies, especially at higher frequencies, that cannot be investigated in the DFR. In this case, we were able to reach frequencies of 2500 Hz and we found excellent acoustic results by employing the porous material associated with the carbon structure.

At system level, it was noticed that the composite materials do not have very high acoustic performances. The trend of the SPL presented peaks in dBA much higher than the aluminum configuration and often, at high frequencies, it exceeded the noise limit. Then, we can deduce that the aluminum has a better performance than the other composite materials. Obviously, the aviation industry always pushes to have increasing lightweight materials and high performance in terms of structural strength. It highlights the fact that it focuses more and more to use composite materials and to improve even more comfort in the cabin. The industry goal is trying to associate sound-absorbing poro-elastic materials to the structure in order to improve the acoustic absorption together to the structural performances.

Indeed, the analyses made show clearly that the best acoustic performances are given by the

fuselage configuration with composite skins and poro-elastic Polyimide core. In this case, the results in terms of SPL are much lower than the noise limit initially fixed. We can conclude that the idea to improve the comfort in the cabin by combining light and strong materials, such as composites and sound-absorbing porous materials can be a good compromise for the development of new regional aircraft concepts.

References

- Arunkumar, M.P., Pitchaimani, J., Gangadharan, K.V. and Babu, M.L. (2016) "Influence of nature of core on vibro acoustic behavior of sandwich aerospace structures", *Aerosp. Sci. Technol.*, **56**, 155-167.
- Beranek, L.L. (1960), *Noise Reduction*, McGraw-Hill Book Company Inc., New York, U.S.A.
- Beranek, L.L. (2007), *The Noisy Dawn of the Jet Age*, *Sound Vib.*, **41**(1), 94-100.
- Beranek, L.L. and Istvan, L.V. (2006), *Noise and Vibration Control Engineering: Principles and Application*, John Wiley and Sons, Inc., New Jersey, U.S.A.
- Bishop, D.E. (1961), "Cruise flight noise levels in a turbojet transport airplane," *Noise Control*, **7**(2), 37-42.
- CleanSky 2 (2014), *Future Trends in Aviation Noise*, Brussel, Belgium, October.
- D'Alessandro, V., Petrone, G., Franco, F. and De Rosa, S. (2013), "A review of the vibroacoustics of sandwich panels: Models and experiments", *J. Sandwich Struct. Mater.*, **15**(5), 541-582.
- Dobrzynski, W. (2010), "Almost 40 years of airframe noise research: What did we achieve?", *J. Aircraft*, **47**(2), 353-367.
- Franco, F., De Rosa, S. and Polito, T. (2011), "Finite element investigations on the vibroacoustic performance of plane plates with random stiffness", *Mech. Adv. Mater. Struct.*, **18**(7), 484-497.
- Hayden, R.E., Murray, B.S. and Theobald, M.A. (1983), "Boundary-layer-induced noise in the interior of aircraft", NASA-CR-172152.
- ICAO (2011), "Annex 16, Vol. 1, Amendment 10", *CAEP/9*, Texas, U.S.A., March.
- ICAO (2013), "Present and Future Trends in Aircraft Noise and Emissions", *Working Paper of Assembly – 38th Session*, Montreal, Canada, July.
- Nichols, R.H., Sleeper, H.P. Jr., Wallace, R.L. Jr. and Ericson, H.L. (1947), "Acoustical materials and acoustical treatments for aircraft," *J. Acous. Soc. Am.*, **19**(3), 428-443.
- Pennig, S., Quehl, J. and Rolny, V. (2012), "Effects of aircraft cabin noise on passenger comfort", *Ergonomics*, **55**(10), 1252-1265.
- Petrone, G., D'Alessandro, V., Franco, F. and De Rosa, S. (2014), "Numerical and experimental investigations on the acoustic power radiated by aluminium foam sandwich panels", *Compos. Struct.*, **118**, 170-177.
- Rayleigh, J.W.S. (1877), *The Theory of Sound*, Macmillan and Co., London, United Kingdom.
- Sagle, A.C. (2014), "Low frequency noise reduction using novel poro-elastic acoustic metamaterials", Ph.D. Dissertation, Virginia Polytechnic Institute and State University, Virginia, U.S.A.
- Sui, N., Yan, X., Huang, T.Y., Xu, J., Yuan, F.G. and Jing, Y. (2015), "A lightweight yet sound-proof honeycomb acoustic metamaterial", *Appl. Phys. Lett.*, **106**(17), 171905.
- Wilby, J.F. (1996), "Aircraft interior noise", *J. Sound Vib.*, **190**(3), 545-564.
- Willshire, W.L. and Stephens, D.G. Jr. (1998), "Aircraft noise technology for the 21st century", *Proceedings of National Conference on Noise Control Engineering*, Michigan, U.S.A, April.
- Workshop Series for Actran 17, Acoustics and Vibroacoustics Training (2016). Free Field Technology, MSC Software Company.
- Yuksel, E., Kamci, G. and Basdogan, I. (2012), "Vibro-acoustic design optimization study to improve the sound pressure level inside the passenger cabin", *J. Vib. Acous-Transactions ASME*, **134**(6), 061017-9.